Received: 4 September 2023 | Accepted: 9 October 2023

DOI: 10.1111/1759-7714.15138

ORIGINAL ARTICLE

WILEY

Circ_0102231 inactivates the PI3K/AKT signaling pathway by regulating the miR-635/NOVA2 pathway to promote the progression of non-small cell lung cancer

Jianhong Liu | **Qiong Yu** | **Xu Yang**

Department of Respiratory Medicine, Zhejiang Jinhua Guangfu Cancer Hospital, Jinhua, China

Correspondence
Qiong Yu, Department of Respiratory Medicine, Zhejiang Jinhua Guangfu Cancer Hospital, Jinhua 321000, China.
Email: krobunc@163.com

Abstract

Background: Circular RNAs (circRNAs) are involved in the malignant development of tumors. However, the mechanism of circ_0102231 in non-small cell lung cancer (NSCLC) has rarely been discussed and reported.

Methods: Quantitative real-time polymerase chain reaction (qRT-PCR) was used to measure the expression of circ_0102231, miR-635 and NOVA alternative splicing regulator 2 (NOVA2) in NSCLC tissues and cells. Western blot was applied to detect the protein expression. Cell proliferation was monitored by cell counting kit-8 (CCK8) and 5-ethynyl-2′-deoxyuridine (EdU) experiments. The angiogenesis ability of cells was tested by angiogenesis assay. Flow cytometry was used to analyze cell apoptosis. The relationship between circ_0102231 and NOVA2 or miR-635 was analyzed by dual-luciferase reporter assay and RNA immunoprecipitation (RIP) assay. An in vivo transplanted tumor model was established to confirm the effect of circ_0102231 on tumor formation.

Results: Circ_0102231 was abnormally upregulated in NSCLC tissues and correlated with clinical stage. Silencing of circ_0102231 inhibited cell proliferation and angiogenesis but significantly promoted the apoptosis of NSCLC cells. There were target binding sites between circ_0102231 and miR-635, miR-635 and NOVA2. Importantly, circ_0102231 acted as a sponge for miR-635, increased the expression of NOVA2, and activated the PI3K/AKT signaling pathway. Finally, silencing of circ_0102231 also had obvious antitumor effects in vivo.

Conclusion: Circ_0102231 increased the expression of NOVA2 by interacting with miR-635 to promote the malignant progression of NSCLC.

KEYWORDS
circ_0102231, miR-635, NOVA2, NSCLC, PI3K/AKT signaling pathway

INTRODUCTION

As a malignant tumor worldwide, lung cancer is characterized by high incidence and poor prognosis.[1] Non-small cell lung cancer (NSCLC) is a histological subtype of lung cancer.[2,3] Although surgery, radiotherapy, chemotherapy and other treatment methods for NSCLC are available, the survival rate is still very low.[4] A better understanding of the mechanisms of action of NSCLC is therefore worth investigating.

Circular RNAs (circRNAs) are endogenous RNAs, which can participate in many cellular functions, such as apoptosis, proliferation, migration and so on.[5–7] CircRNAs have better stability than linear genes because they form covalently closed continuous rings through back splicing without 3′ or 5′ end.[8] CircRNAs are regarded as a biomarker for the effective diagnosis of cancer.[9] MicroRNA (miRNA) contains about 22 nucleotides.[10] More and more studies have shown that circRNAs have complementary binding sites of miRNA, which regulate gene transcription by acting as effective miRNA sponges and effective competitive endogenous RNAs (ceRNAs).[11] For example, circ_0091570 suppresses hepatocellular cancer progression by sponging miR-1307[12]; Circ_0102049 promotes

osteosarcoma cell progression through sponging miR-1304 and targeting MDM2[13]; circ0037128/miR-17-3p/AKT3 axis promotes the occurrence of diabetic nephropathy, and so on.[14] In previous studies, circ_0102231 was found to be abnormally elevated in NSCLC,[15] but the research was not particularly sufficient. Therefore, this study chose circ_0102231 as the research object to further explore its function and mechanism.

In the present study we aimed to clarify circ_0102231 function in NSCLC. In terms of function, circ_0102231 promoted NSCLC cell proliferation and angiogenesis. In terms of mechanism, circ_0102231 regulated miR-635/NOVA alternative splicing regulator 2 (NOVA2) axis and PI3K/AKT signaling pathway.

METHODS

Tissues and cell lines

Lung tissues were obtained from Zhejiang Jinhua Guangfu Cancer Hospital with the support of the ethics committee of this hospital. No patient had radiotherapy or chemotherapy before surgery, and all patients signed their informed consent. After tissues were removed, they were stored immediately at − 80°C.

Human NSCLC cell lines (A549, H1299, and H1581) and normal bronchial epithelial cells (BEAS-2B cells) were acquired from the Chinese Academy of Sciences (Shanghai, China). Cells were all grown in RPMI-1640 medium (Solarbio), which contained 10% fetal bovine serum (FBS), in an incubator containing 5% CO_2 at 37°C.

Quantitative real-time polymerase chain reaction (qRT-PCR)

TriQuick reagent (Solarbio) and NanoDrop 2000c (Thermo Fisher Scientific) were applied to extract RNA and evaluate RNA quality, respectively. cDNA was obtained with the cDNA synthesis kit (Takara). Finally, circ_0102231, miR-635, and NOVA2 were quantified with SYBR Mix (Toyobo Co.) and the corresponding primers are shown in Table 1. U6 and GAPDH were regarded as internal parameters and $2^{-\Delta\Delta CT}$ method was used for analysis.

Subcellular fractionation location assay

The cytoplasmic and nuclear circ_0102231 was analyzed as instructed by the manufacturer of the PARIS kit (Thermo Fisher). Circ_0102231 expression was quantified by qRT-PCR.

Cell transfection

SiRNAs and shRNA for circ_0102231 (si-circ_0102231 and sh-circ_0102231), siRNA negative control and shRNA negative control (si-NC and sh-NC), miR-635 mimic, miR-635 inhibitor and their controls, NOVA2 overexpression plasmid (NOVA2) were purchased from Ribobio. Lipofectamine 3000 (Thermo Fisher Scientific) was selected for cell transfection.

TABLE 1 Primer sequences used for polymerase chain reaction (PCR).

Name	Primers for PCR (5′–3′)	
hsa_circ_0102231	Forward	CTGCTAAGGAGTGTGTTTTGGT
	Reverse	ATTCTGTGGAAGATCTGGAAGC
NOVA2	Forward	GCAAGAGGCCCCTCGAAAC
	Reverse	AGCTTGATCTCGTCCGTTCC
miR-635	Forward	GCCGAGACTTGGGCACTGAAACA
	Reverse	AGTGCAGGGTCCGAGGTATT
GAPDH	Forward	AGCTCACTGGCATGGCCTTC
	Reverse	CGCCTGCTTCACCACCTTCT
U6	Forward	CGCTTCACGAATTTGCGTGTCAT
	Reverse	GCTTCGGCAGCACATATACTAAAAT
KIAA0586	Forward	ATGAGACTGTAGAGCGGTCTTG
	Reverse	TGACCTCAGAGCCCAAAACAT

Cell proliferation assays

For the cell counting kit-8 (CCK-8) experiment, cells were transfected and inoculated into 96-well plates according to the experimental requirements. At specific time points (0, 24, 48, and 72 h), cells in each well were mixed with of CCK8 solution (10 μL, Sigma) and cultured in an incubator for 4 h. The absorbance was measured at 450 nm.

For the 5-ethynyl-2′-deoxyuridine (EdU) assay, cells (1×10^5 cells/well) were seeded into 96-well plates. The proliferation of transfected cells was detected according to the manufacturer's instructions of the EdU kit (KeyGen). Nuclei were stained with 4′,6-diamidino-2-phenylindole (DAPI).

Tube formation assay

The experiment was carried out in 96-well plates. Matrigel (BD Biosciences) was placed in the orifice plate and allowed to set at 37°C. The supernatants of NSCLC cells were collected and used to incubate human umbilical vein endothelial cells (HUVEC) Then, the cells were seeded in plates. Five hours later, the formation of a pipeline was observed and was photographed under a microscope (Nikon) and analyzed with ImageJ software.

Cell apoptosis assay

The cells were transfected according to the manufacturer's instructions (KeyGEN). 1×10^4 A549 or H1299 cells were used for this assay. With the addition of 5 μL annexin V-FITC and 5 μL PI, the mixture was reacted at room

temperature without light for 15 min. Then, a flow cytometer (BD Biosciences) was used to assess cell apoptosis.

Western blot analysis

Transfected cells were lysed and separated by 10% SDS-PAGE. The membrane was sealed with 5% nonfat milk powder for 1 h and then immunoblotted with the following antibodies at 4°C for 12 h. Afterwards, the secondary antibodies of the corresponding species were incubated with membrane. Finally, an enhanced chemiluminescence (ECL) detection system (Thermo Fisher) was applied to visualize the bands. The antibodies were: anti-PCNA (ab92552, Abcam), anti-NOVA2 (PA5-69076, Thermo Fisher), anti-p-PI3K (ab278545, Abcam), anti-p-AKT (ab38449, Abcam), anti-PI3K (ab32089, Abcam), anti-AKT (ab18785, Abcam), anti-Bax (ab182734, Abcam), anti-Bcl-2 (ab182858, Abcam), and anti-GAPDH (ab181602, Abcam).

Dual-luciferase reporter gene assay

The wild and mutated sequences of circ_0102231 and NOVA2 were obtained from Promega and then inserted into pmirGLO vector. NSCLC cells were cotransfected with the above vectors and miR-635 or miR-NC. After 48 h of transfection, luciferase activities were tested using a luciferase reporter assay kit (Promega).

RNA immunoprecipitation (RIP)

A Magna RNA immunoprecipitation kit (Millipore) was used for this assay. Cells were lysed with RIP lysis buffer. The lysate was incubated with argonaute-2 (Ago2) antibody

TABLE 2 Association of circ_0102231 expression with clinicopathological features of non-small cell lung cancer (NSCLC) patients.

Features	*n*	circ_0102231 expression		*p*-value
		High ($n = 17$)	Low ($n = 16$)	
Age (years)				
≥60	22	10	12	0.325
<60	11	7	4	
Gender				
Male	19	12	7	0.119
Female	14	5	9	
Tumor node metastasis (TNM) stage				
I–II	13	3	10	0.008
III	20	14	6	
Lymph node metastasis				
Yes	18	13	5	0.009
No	15	4	11	
Distant metastasis				
Yes	10	9	1	0.004
No	23	8	15	

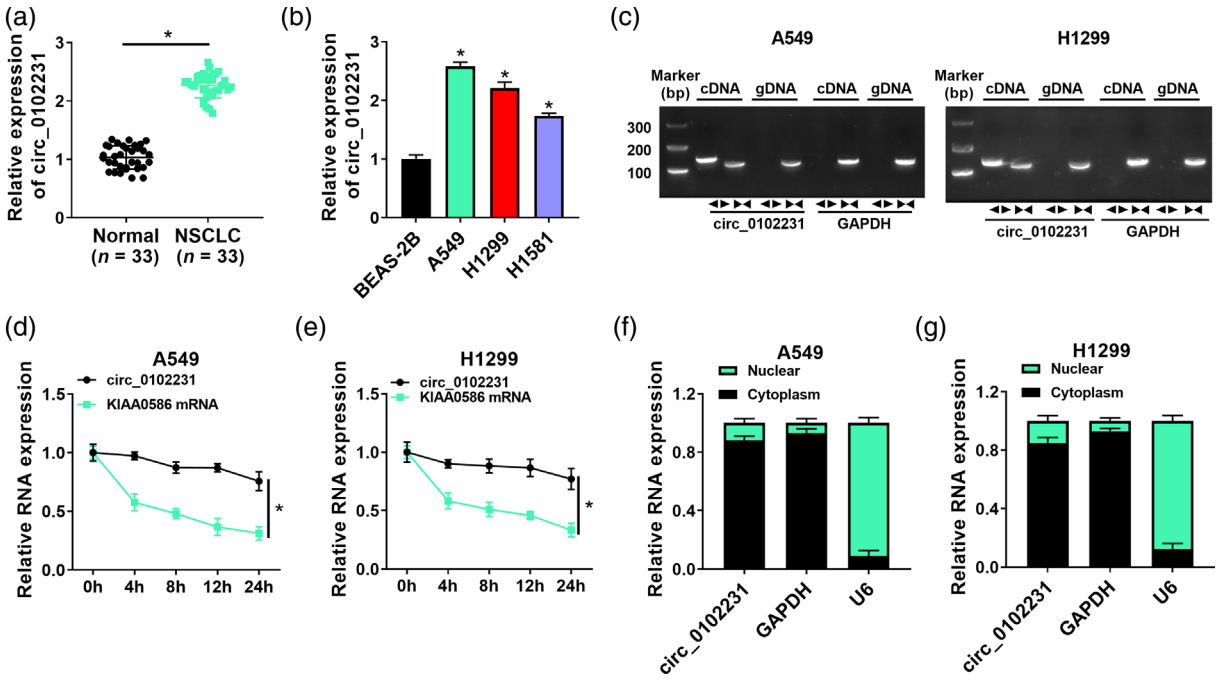

FIGURE 1 High expression of circ_0102231 in non-small cell lung cancer (NSCLC). (a) Relative circ_0102231 expression in NSCLC tumor tissues compared with adjacent normal tissues ($n = 33$) were determined by quantitative real-time polymerase chain reaction (qRT-PCR). (b) Relative circ_0102231 expression in NSCLC cell lines was measured by qRT-PCR. (c–e) The ring characteristic of circ_0102231 was analyzed using divergent primers, convergent primers and actinomycin (d). (f, g) The location of circ_0102231 in NSCLC cells was analyzed by subcellular fractionation location assay. Data are presented as mean ± SD. $^*p < 0.05$.

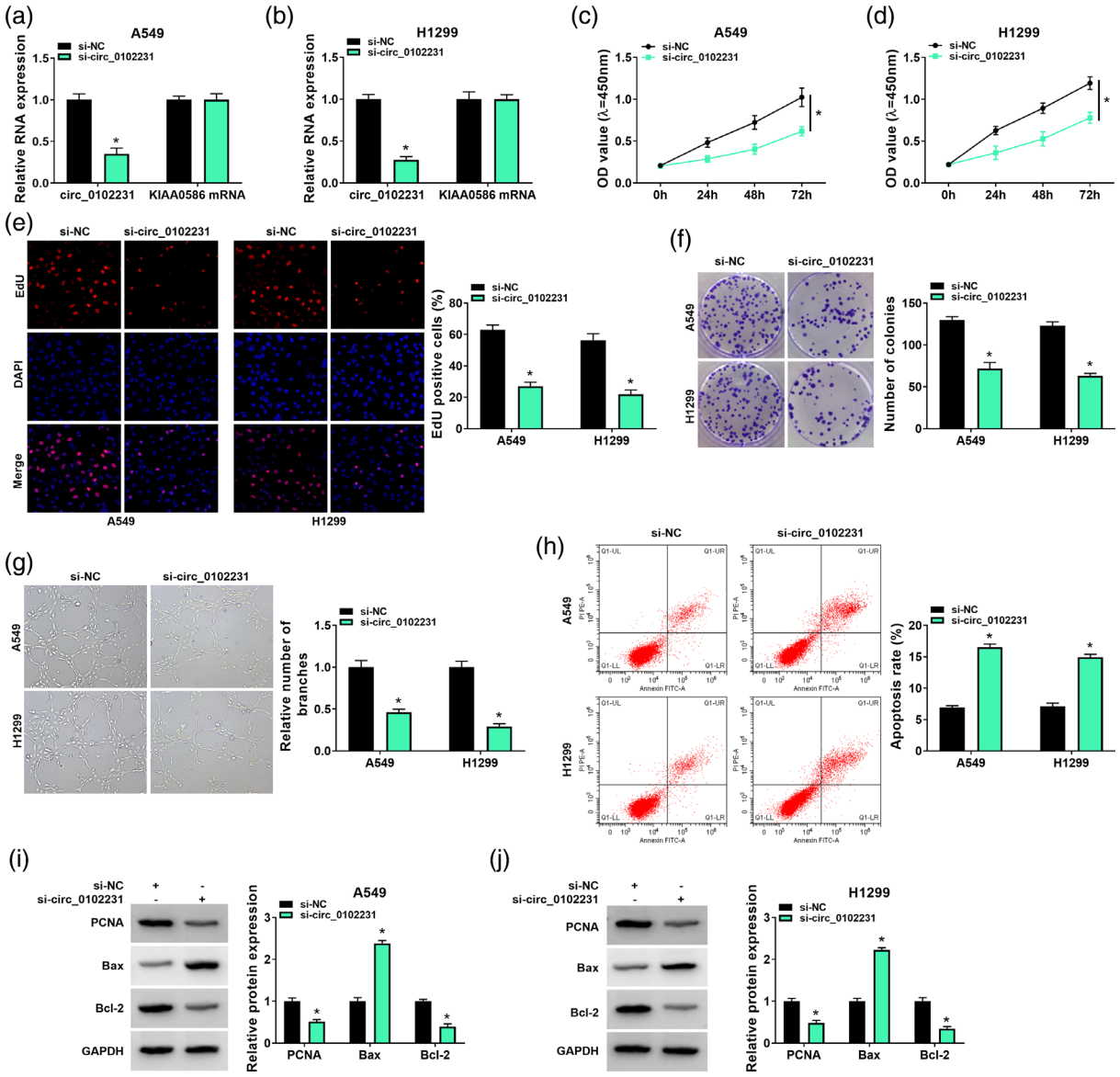

FIGURE 2 Effects of circ_0102231 on non-small cell lung cancer (NSCLC) progression in vitro. (a, b) Relative circ_0102231 expression in A549 and H1299 cells with the transfection of si-circ_0102231 or siRNA negative control (si-NC). Cell counting kit-8 (CCK-8) assays (c, d), 5-ethynyl-2′-deoxyuridine (EdU) assays (e) and colony formation assays (f) were performed to evaluate the proliferation of A549 and H1299 cells. (g) The angiogenic ability of cells was detected by angiogenesis experiment. (h) The apoptosis rate was measured via flow cytometry. (i, j) The protein level of PCNA, Bax and Bcl-2 was examined using western blot. Data are presented as mean ± SD. *$p < 0.05$.

and IgG antibody (Abcam), respectively. Sepharose beads were then added and incubated with the mixture overnight at 4°C. Finally, RNA was detected by qRT-PCR.

Mouse model studies

All in vivo experiments were authorized by the Ethics Committee of Zhejiang Jinhua Guangfu Cancer Hospital and performed in accordance with the guidelines of the National Animal Care and Ethics Institution. Ten BALB/c nude mice (5-week-old), all female, were purchased from Hunan Slyke Jingda Experimental Animal Co., Ltd (Changsha, China). Cell suspensions stably transfected with sh-NC and sh-circ_0102231 were injected into the right back of mice to form tumors. The length and width of tumor were measured weekly and calculated according to the formula: $1/2 \times a \times b^2$ (a: length; b: width). After 28 days, the tumor tissues were removed, measured, and weighed, and fixed with 4% paraformaldehyde.

Immunohistochemistry (IHC)

The fixed tumor tissue was dehydrated and sectioned (4 μm). After blocking the endogenous catalase, the antigen was

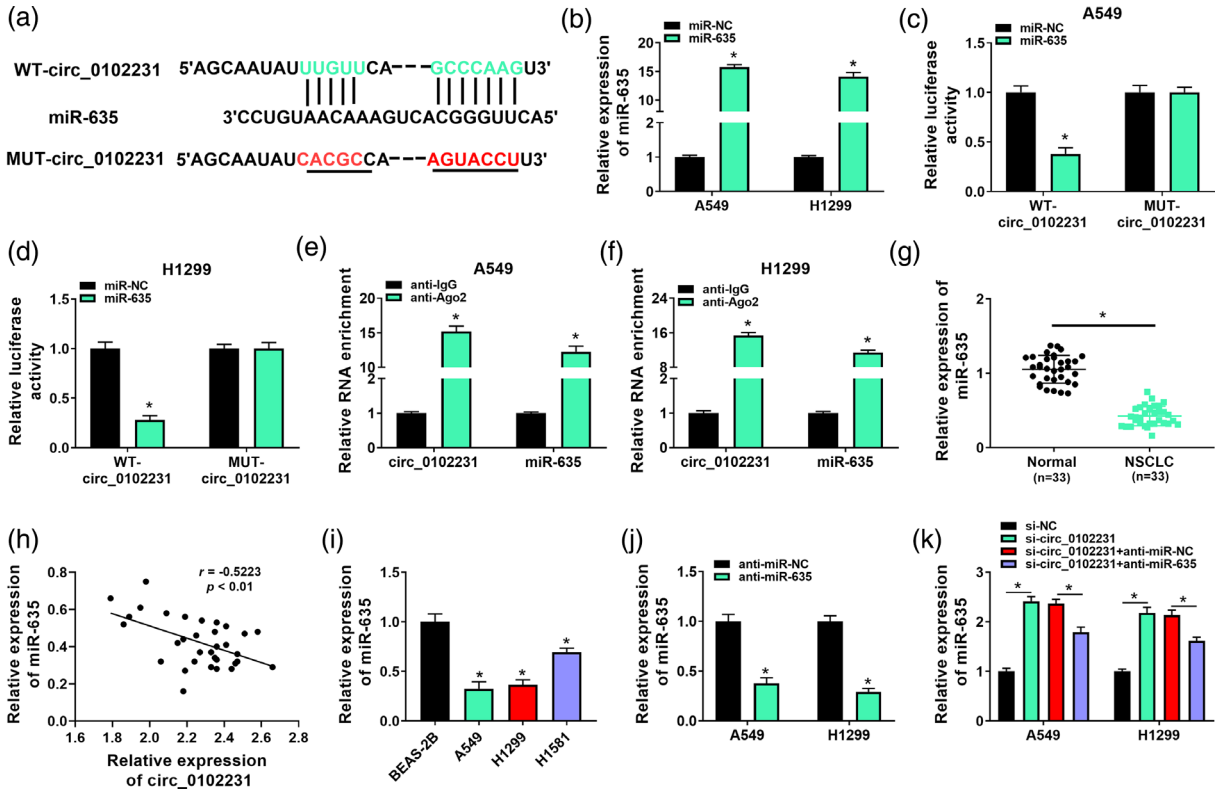

FIGURE 3 Circ_0102231 acted as a molecular sponge for miR-635. (a) Circular RNA Interactome predicted that circ_0102231 and miR-635 had targeted binding sites. (b) Transfection efficiency of miR-635 mimic was tested by quantitative real-time polymerase chain reaction (qRT-PCR). (c, d) Luciferase activity was detected in non-small cell lung cancer (NSCLC) cells cotransfected with WT-circ_0102231 or MUT-circ_0102231 and miR-NC or miR-635. (e, f) The correlation between circ_0102231 and miR-635 were confirmed by RIP assay. (g) MiR-635 level was measured in NSCLC tissues and adjacent noncancer tissues. (h) The correlation of miR-635 and circ_0102231 was analyzed by Spearman correlation analysis in NSCLC tissues. (I) MiR-635 level was detected in BEAS-2B, A549, H1299 and H1581 cells. (J) Transfection efficiency of miR-635 inhibitor was checked by qRT-PCR. (k) MiR-635 expression was measured in A549 and H1299 cells introduced with siRNA negative control (si-NC), si-circ_0102231, si-circ_0102231 + anti-miR-NC or si-circ_0102231 + anti-miR-635. Data are presented as mean ± SD. $^*p < 0.05$.

exposed by heating. Ki67 antibody (ab15580, Abcam) was incubated with the sections overnight. Appropriate secondary antibody was incubated with the sections for 1.5 h. Representative photographs were taken under the microscope, and the positive cell rate in the visual field was calculated.

Statistical analysis

The data from three independent experiments were recorded as mean ± SD. Statistical analysis was conducted using Graphpad prism 7. Student's *t*-test or two-way analysis of variance (ANOVA) was utilized to analyze two or more groups of data. *p*-values < 0.05 were deemed statistically significant.

RESULTS

High expression of circ_0102231 in NSCLC

A total of 33 pairs of adjacent and cancerous tissues were collected for this study. As shown in Figure 1a, the expression of circ_0102231 was abnormally elevated in NSCLC tissues. In addition, circ_0102231 expression was significantly associated with TNM stage, lymph node metastasis and distant metastasis of NSCLC (Table 2). In NSCLC cells, the expression of circ_0102231 was also significantly increased (Figure 1b). Circ_0102231 was only amplified in cDNA using divergent primers (Figure 1c). As shown in Figure 1d,e, after actinomycin D treatment, the expression of circ_0102231 did not change strikingly, but the mRNA expression of linear transcript KIAA0586 was obviously decreased. Further, circ_0102231 was mainly expressed in the cytoplasm of the A549 and H1299 cells (Figure 1f,g). These results indicated that circ_0102231, which has a stable ring structure, was highly expressed in NSCLC, and was related to clinical stage.

Effects of circ_0102231 on NSCLC progression in vitro

According to the results in Figure 1, the expression of circ_0102231 was higher in A549 and H1299 cells. The two cells were used for in vitro study. First, we detected

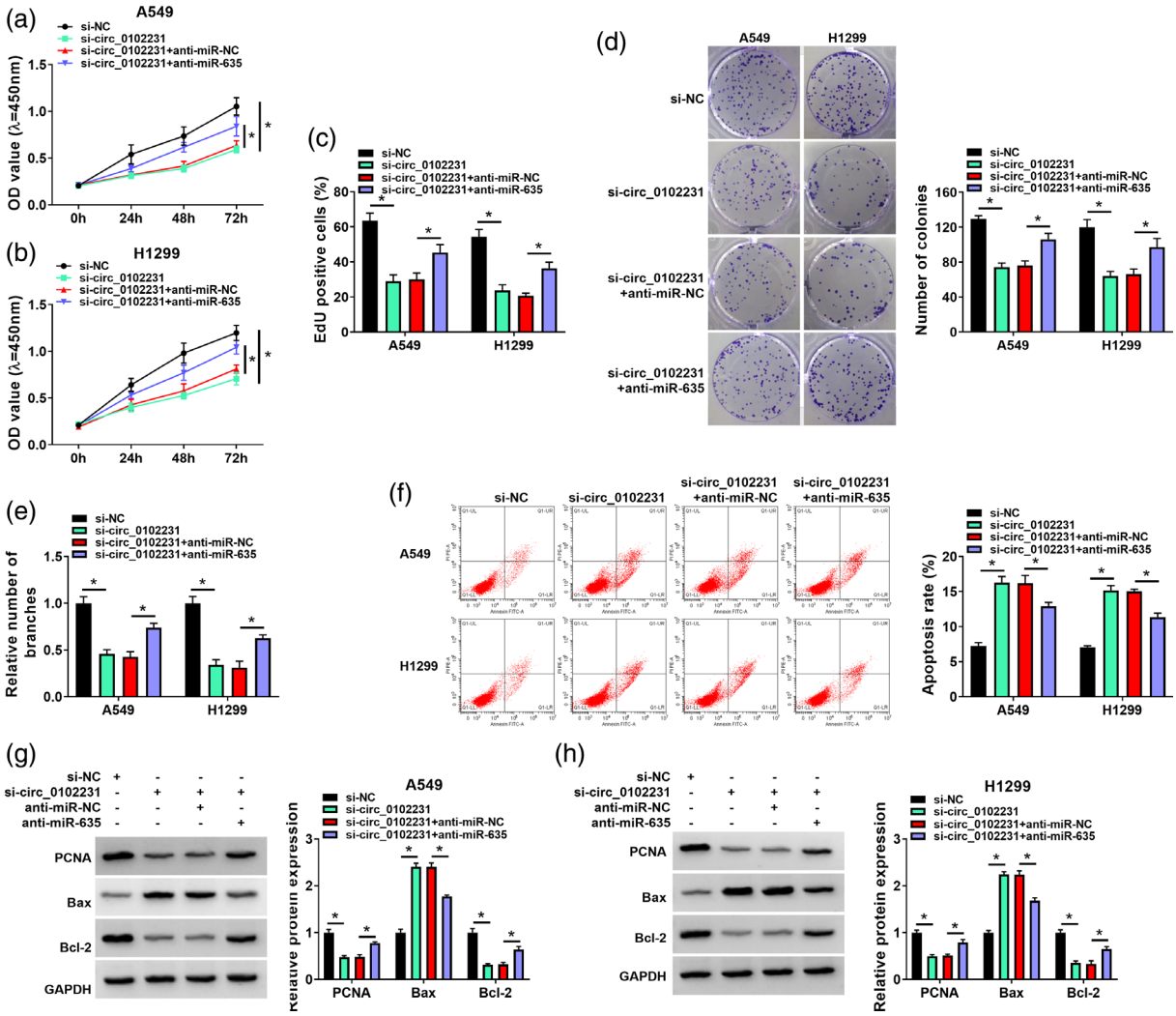

FIGURE 4 MiR-635 knockdown partly abolishes si-circ_0102231 induced effects in NSCLC cells. A549 and H1299 cells were transfected with si-NC, si-circ_0102231, si-circ_0102231 + anti-miR-NC, or si-circ_0102231 + anti-miR-635. CCK8 assays (a, b), 5-ethynyl-2′-deoxyuridine (EdU) assays (c) and clone formation experiments (d) were used to detect cell proliferation. (e) The ability of cells to form blood vessels was assessed by tube formation assay. (f) Apoptosis was detected by flow cytometry. (g, h) The protein levels of PCNA, Bax and Bcl-2 were detected by western blot. Data are presented as mean ± SD. $^*p < 0.05$.

the interference efficiency of si-circ_0102231. Compared with the control group, the expression of circ_0102231 was significantly reduced after transfection with si-circ_0102231, but the expression of its linear gene was not affected (Figure 2a,b). CCK8 and EdU experiments confirmed the inhibitory effect of silencing of circ_0102231 on cell proliferation (Figure 2c–e). Similarly, in the plate clone formation experiment, silencing of circ_0102231 also showed a certain inhibitory effect on cell clone formation (Figure 2f). At the same time, silencing of circ_0102231 significantly reduced angiogenesis but promoted cell apoptosis (Figure 2g,h). As shown in Figure 2i,j the expression of PCNA and Bcl-2 decreased after interfering with circ_0102231, while the expression of Bax increased. In conclusion, silencing of circ_0102231 inhibited tumor progression in vitro.

Circ_0102231 acted as a molecular sponge for miR-635

In depth, we explored the regulatory mechanism of circ_0102231. Based on the bioinformatic database Circinteractome, Figure 3a shows the binding sites of circ_0102231 and miR-635. The transfection efficiency of miR-635 is verified in Figure 3b. In order to verify the binding of circ_0102231 and miR-635, we carried out a dual luciferase reporter assay. In A549 and H1299 cells, the luciferase activity of WT-circ_0102231 was notably inhibited by miR-635 overexpression (Figure 3c,d). In addition, a RIP assay was also used to verify the binding of circ_0102231 and miR-635. IgG group was used as the control group, and the results indicated that circ_0102231 and miR-635 were enriched in Ago2-immunoprecipitated complexes (Figure 3e,f). Contrary

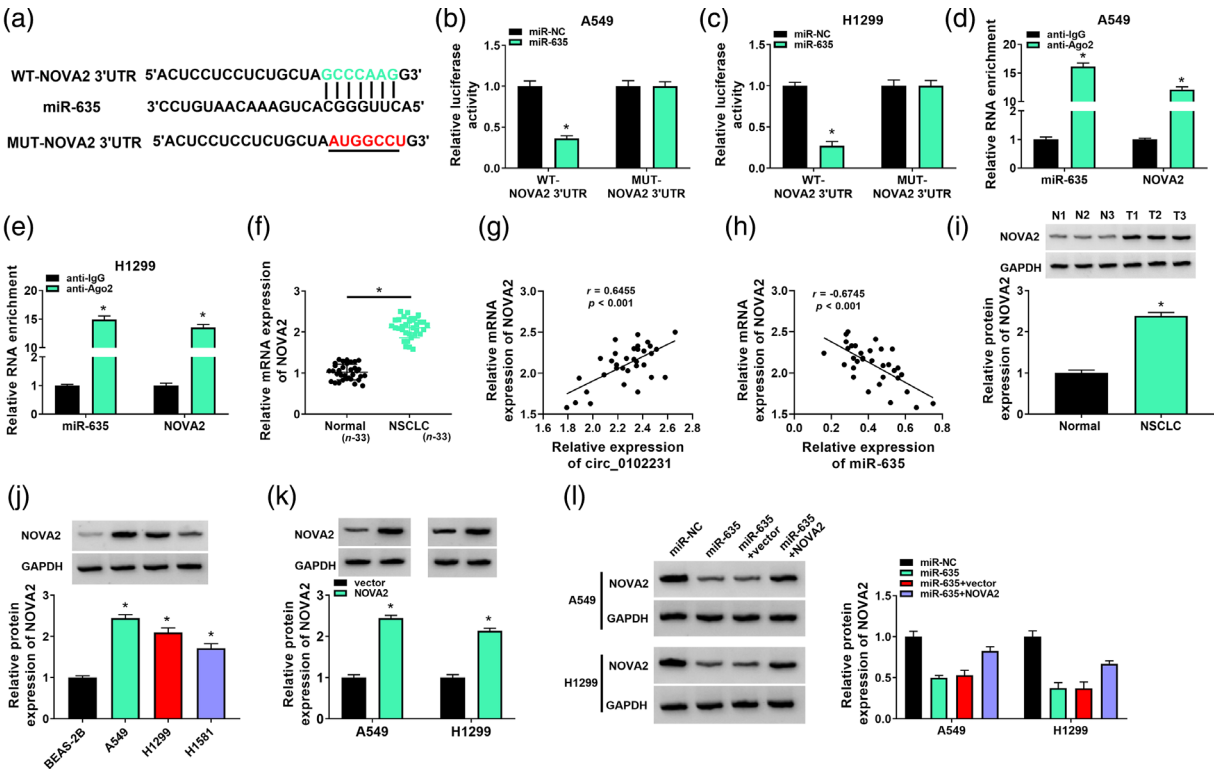

FIGURE 5 MiR-635 directly interacts with the 3′UTR of NOVA alternative splicing regulator 2 (NOVA2) in non-small cell lung cancer (NSCLC) cells. (a) The putative target sites between miR-635 and NOVA2 were predicted by starBase. (b, c) Luciferase activity was detected in NSCLC cells cotransfected with WT-NOVA2 3′UTR or MUT-NOVA2 3′UTR and miR-NC or miR-635. (d, e) The enrichment of miR-635 or NOVA2 was measured by RNA immunoprecipitation (RIP) assay in NSCLC cells. (f) The mRNA of NOVA2 was measured in NSCLC tissues and adjacent noncancer tissues. (g, h) The correlation of NOVA2 with circ_0102231 and miR-635 was analyzed by Spearman correlation analysis in NSCLC tissues. (i, j) The protein expression of NOVA2 was detected in NSCLC tissues, normal lung tissues, BEAS-2B cells, A549 cells, H1299 cells, and H1581 cells. (k) The transfection efficiency of NOVA2 overexpression plasmid was analyzed by western blot. (l) NOVA2 expression was measured in A549 and H1299 cells introduced with miR-NC, miR-635, miR-635 + vector, or miR-635 + NOVA2. Data are presented as mean ± SD. $^*p < 0.05$.

to the expression of circ_0102231 in NSCLC tissues and cells, the expression of miR-635 in NSCLC tissues was decreased (Figure 3g). MiR-635 expression was negatively correlated with circ_0102231 expression in NSCLC tissues (Figure 3h). As shown in Figure 3i, miR-635 expression was downregulated in NSCLC cells (A549, H1299 and H1581) when compared with BEAS-2B cells. The inhibitor efficiency of miR-635 is verified in Figure 3j. Interference with circ_0102231 promoted the expression of miR-635, while anti-miR-635 partially alleviated the increase of miR-635 (Figure 3k). In brief, circ_0102231 reduced the expression of miR-635 in NSCLC cells by sponging miR-635.

MiR-635 knockdown partly abolished si-circ_0102231 induced effects in NSCLC cells

Next, we carried out rescue experiments to explore the effect of miR-635 on the function of circ_0102231. Circ_0102231 interference inhibited the proliferation (Figure 4a–d) and angiogenesis (Figure 4e) but promoted cell apoptosis (Figure 4f). Moreover, the addition of anti-miR-635 restored these functions of circ_0102231 knockdown on NSCLC cells (Figure 4a–f). In addition, the levels of PCNA and Bcl-2 protein in NSCLC cells were decreased significantly with the silencing of circ_0102231, while the Bax level was increased. However, these effects were weakened by the introduction of anti-miR-635 (Figure 4g,h). These data indicated that the circ_0102231/miR-635 axis was engaged in NSCLC progression.

MiR-635 directly interacted with the 3′UTR of NOVA2 in NSCLC cells

According to the prediction of TargetScan, NOVA2 is the downstream target of miR-635, and the binding site is shown in Figure 5a. To verify the binding of miR-635 and NOVA2, we performed luciferase reporter analysis in NSCLC cells. We observed that the luciferase activity of cells transfected with wild-type NOVA2 3′UTR vector (WT-NOVA2 3′UTR) rather than mutant NOVA2 3′UTR vector (MUT-NOVA2 3′UTR) was significantly reduced by cotransfection of miR-635 mimic, indicating that NOVA2 is the target of miR-635 (Figure 5b,c). RIP analysis showed that miR-635 and NOVA2 were enriched in Ago2-immunoprecipitated complexes in comparison with IgG, suggesting that both miR-635 and NOVA2 could bind to

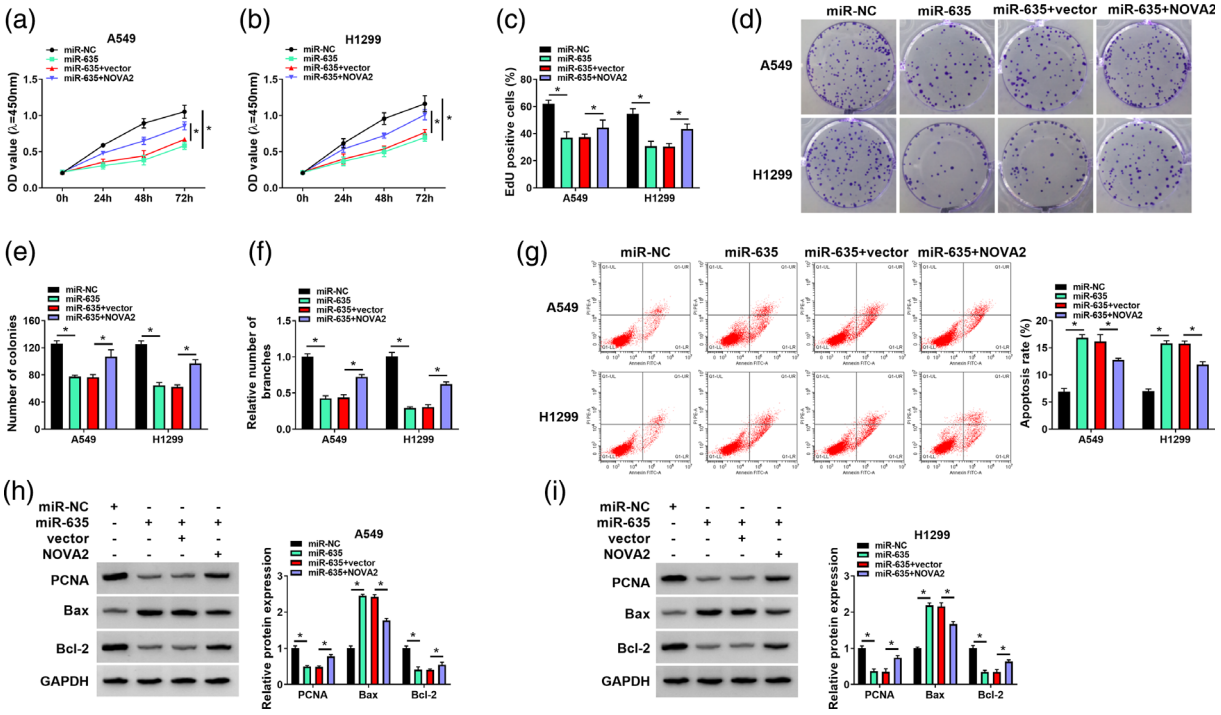

FIGURE 6 Overexpression of NOVA alternative splicing regulator 2 (NOVA2) also led to recovery of cellular malignant phenotypes after upregulation of miR-635. A549 and H1299 cells were transfected with miR-NC, miR-635, miR-635 + vector, or miR-635 + NOVA2. CCK8 assays (a, b), 5-ethynyl-2′-deoxyuridine (EdU) assays (c) and clone formation experiments (d) were used to detect cell proliferation. (f) The angiogenic ability of HUVEC was illustrated by tube formation experiments. (g) Apoptosis of A549 and H1299 cells was detected by flow cytometry. (h, i) The protein levels of PCNA, Bax and Bcl-2 were measured by western blot. Data are presented as mean ± SD. $^*p < 0.05$.

RNA-induced silencing complex (Figure 5d,e). We continued to monitor the expression of NOVA2, which was significantly increased in NSCLC tissues (Figure 5f). NOVA2 expression was positively correlated with circ_0102231 expression but negatively with miR-635 expression in NSCLC tissues (Figure 5g,h). Furthermore, NOVA2 protein expression was upregulated in NSCLC tissues and cells relative to normal controls (Figure 5i,j). The regulatory relationship between miR-635 and NOVA2 was verified. Compared with the vector group, the expression of NOVA2 in cells transfected with NOVA2 overexpression vector was sharpened significantly (Figure 5k). The expression of NOVA2 was decreased significantly in the miR-635 group, and this trend was reversed after transfection of NOVA2 (Figure 5l). The above results showed that NOVA2 was the targeted binding site of miR-635 and was negatively regulated by miR-635.

Overexpression of NOVA2 reversed the effects of miR-635 overexpression on the malignant phenotypes of NSCLC

To further explore the relationship between miR-635 and NOVA2 in NSCLC cells, we transfected cells with miR-NC, miR-635, miR-635 + vector and miR-635 + NOVA2. The inhibitory effect of miR-635 on cell proliferation and angiogenesis and the promotion effect of miR-635 on apoptosis were partially reversed by the introduction of NOVA2 (Figure 6a–g). For function related marker proteins, the expression of PCNA and Bcl-2 were decreased, while the expression of Bax was increased after miR-635 transfection, whereas these effects were overturned with the introduction of NOVA2 (Figure 6h,i). These results demonstrated that the suppressive role of miR-635 knockdown in NSCLC progression could be reversed by NOVA2 overexpression.

NOVA2 acted as the downstream target gene of circ_0102231/miR-635

Next, we explored the relationship between circ_0102231, miR-635 and NOVA2. In A549 cells, the mRNA and protein expression of NOVA2 were decreased after silencing of circ_0102231, and this reduction tendency was attenuated by the introduction of anti-miR-635 (Figure 7a,b). This regulatory trend was confirmed again in H1299 cells (Figure 7c,d). The above results showed that circ_0102231 regulated the expression of NOVA2 through miR-635.

Circ_0102231 regulated the PI3K/AKT signaling pathway by interacting with miR-635 in NSCLC cells

In order to explore the effect of circ_0102231 on PI3K/AKT signaling pathway, the protein levels of p-PI3K, total

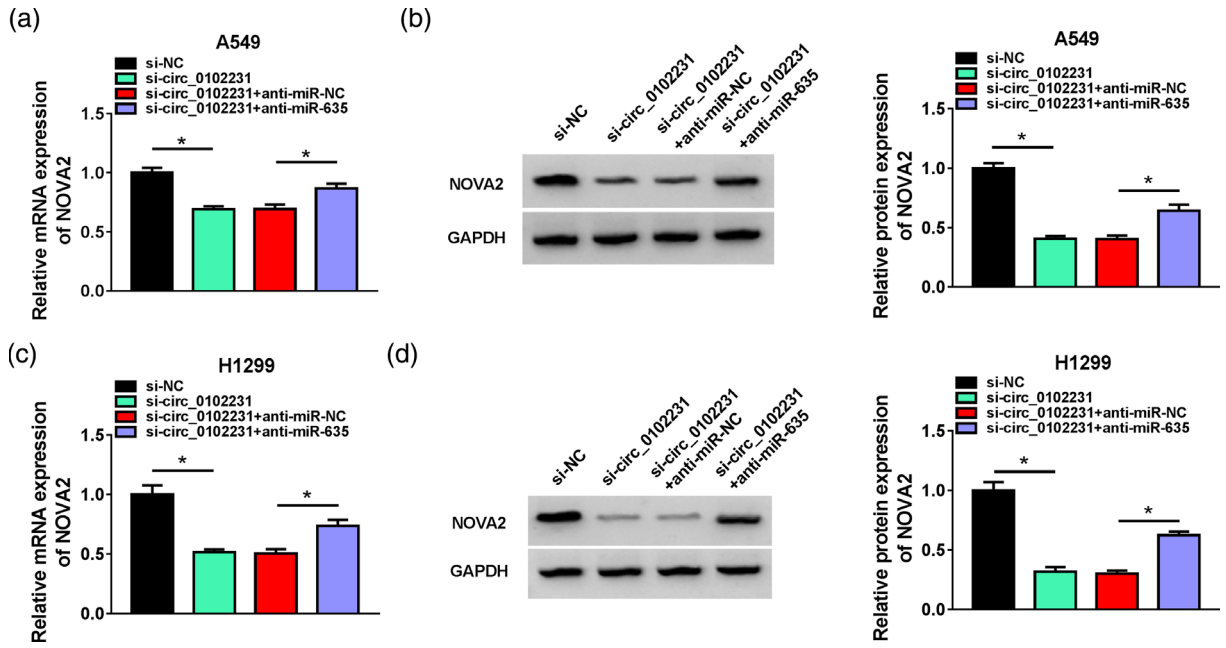

FIGURE 7 NOVA alternative splicing regulator 2 (NOVA2) acted as the downstream target gene of circ_0102231/miR-635. A549 and H1299 cells were transfected with si-NC, si-circ_0102231, si-circ_0102231 + anti-miR-NC, or si-circ_0102231 + anti-miR-635. (a, b) The mRNA and protein levels of NOVA2 in A549 cells were measured by quantitative real-time polymerase chain reaction (qRT-PCR) and western blot. (c, d) qRT-PCR and western blot was conducted to detect the mRNA and protein levels of NOVA2 in H1299 cells, respectively. Data are presented as mean ± SD. $^*p < 0.05$.

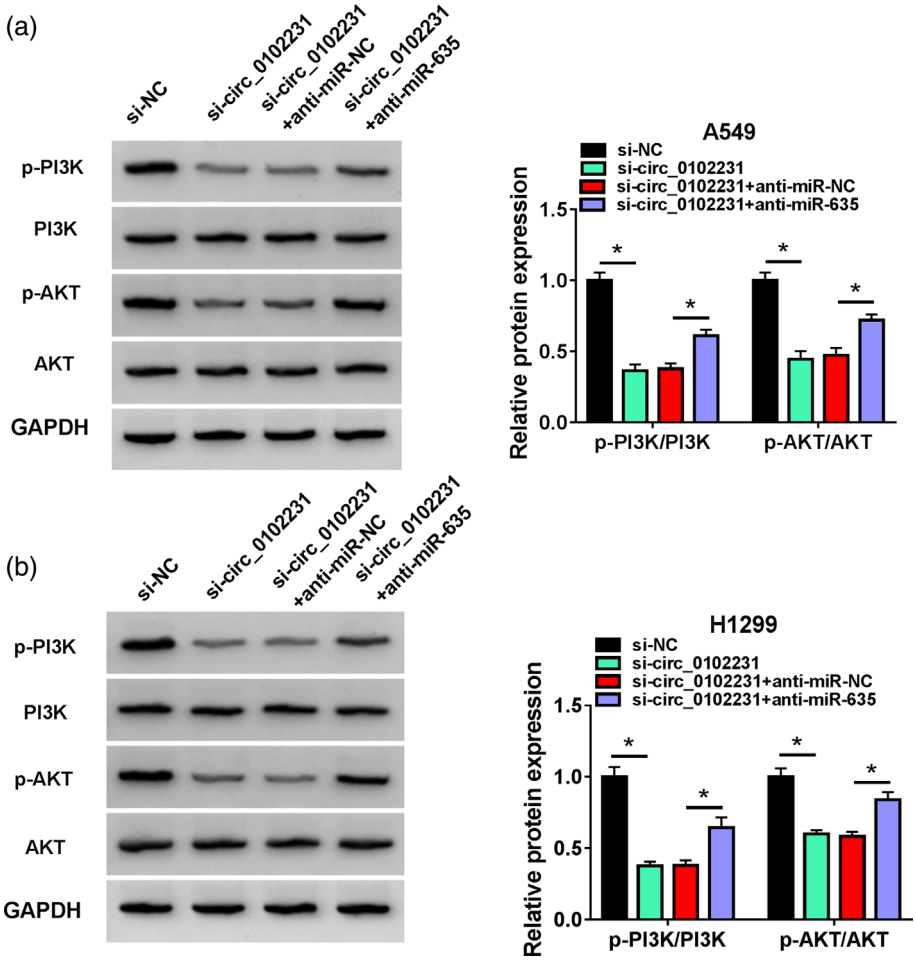

FIGURE 8 Circ_0102231 regulates the PI3K/AKT signaling pathway by interacting with miR-635 in NSCLC cells. A549 and H1299 cells were transfected with si-NC, si-circ_0102231, si-circ_0102231 + anti-miR-NC or anti-miR-635 (a) The protein levels of p-PI3K, PI3K, p-AKT and AKT in A549 cells were assessed using western blot assays. (b) Western blot assays were used to detect the protein levels of p-PI3K, PI3K, p-AKT, and AKT in H1299 cells. Data are presented as mean ± SD. $^*p < 0.05$.

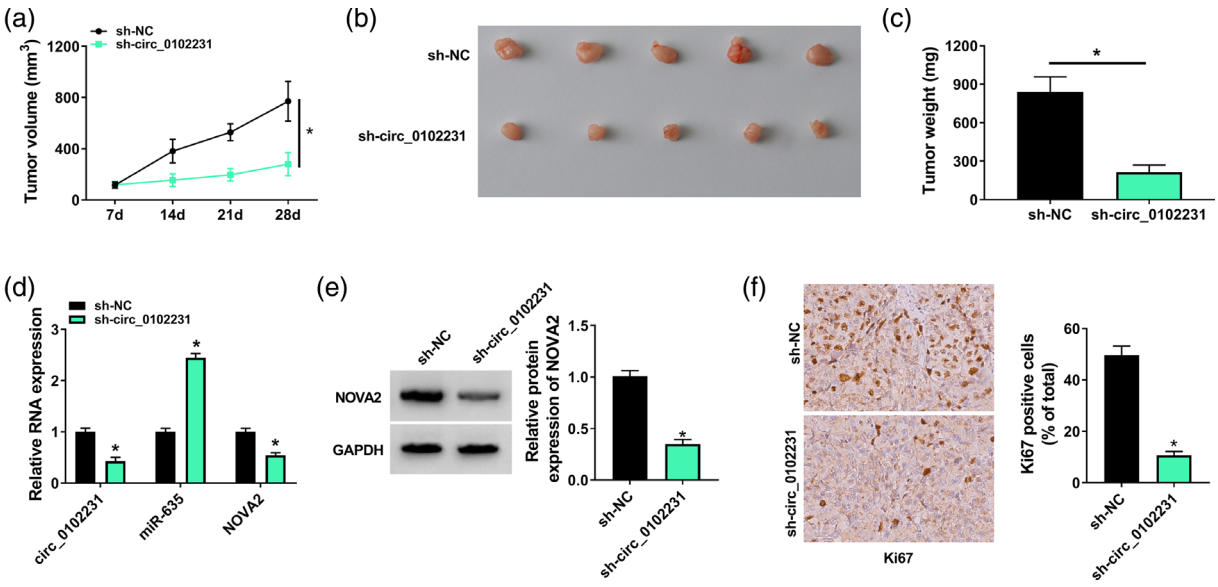

FIGURE 9 Effects of circ_0102231 on non-small cell lung cancer (NSCLC) growth in vivo. (a) Tumor growth curve of nude mice. (b) Tumor formation shown in nude mice at 28 days. (c) Tumor weight in nude mice at 28 days. (d, e) The levels of circ_0102231, miR-635 and NOVA2 in xenograft tumors were tested using quantitative real-time polymerase chain reaction (qRT-PCR) or western blot. (f) The immunohistochemical detection of Ki67 in tumor tissues of nude mice. Data are presented as mean ± SD. $^*p < 0.05$.

PI3K (PI3K), p-AKT, total AKT (AKT) in si-NC, si-circ_0102231, si-circ_0102231 + anti-miR-NC and si-circ_0102231 + anti-miR-635 group in NSCLC cells were detected. The results showed that in the si-circ_0102231 group, the protein levels of p-PI3K and p-AKT were significantly downregulated, the levels of PI3K and AKT did not change significantly, and the situation was reversed after anti-miR-635 infection (Figure 8a,b). In conclusion, these results suggested that the circ_0102231/miR-635 axis regulated the PI3K/AKT signaling pathway in NSCLC.

Effects of circ_0102231 on NSCLC growth in vivo

Sh-NC and sh-circ_0102231 were stably transfected into A549 cells, and the xenograft tumor model in nude mice was established. As presented in Figure 9a, a slow growth of tumor volume was observed in the sh-circ_0102231 group. The tumor volume and weight were lower than those in sh-NC group (Figure 9b,c). In addition, we also observed that compared with the sh-NC group, the expression of circ_0102231 and NOVA2 in tumor tissues of the sh-circ_0102231 group was downregulated, while the expression of miR-635 was upregulated (Figure 9d,e). Immunohistochemical staining indicated that silencing of circ_0102231 significantly decreased the positive expression of Ki67 in tumor tissues of nude mice (Figure 9f). The above results revealed that circ_0102231 knockdown also inhibited tumor growth in vivo.

DISCUSSION

CircRNAs were first proposed in the 1970s.[16] As reported, circRNA can be involved in multiple cancers, which mainly regulates gene expression by acting as a sponge of miRNAs.[17–19] NSCLC patients account for 70% of all lung cancer patients.[20] At present, many circRNAs have been confirmed to be involved in the progress of NSCLC, such as circLDB2,[21] and circ_0058357.[22] From the existing studies,[15] we selected circ_0102231 as the research object to further reveal its function and mechanism in NSCLC. We demonstrated that circ_0102231 was abnormally expressed in NSCLC. To investigate the function of circ_0102231, we transfected small interfering RNA of circ_0102231 into NSCLC cells and reduced its expression. Silencing of circ_0102231 could significantly repress the progression of NSCLC. In addition, silencing of circ_0102231 also showed a certain inhibitory effect on the growth of tumors in vivo.

Next, the circRNA-miRNA-mRNA regulatory network of circ_0102231 was discussed. Based on the online prediction website circular RNA interactome, we found the miR-635 was the downstream target of circ_0102231 and verified their binding relationship. The function of miR-635 in NSCLC has been previously discussed. Zhang et al. proved that miR-635 was identified as an effective cell invasion inhibitor and differentially expressed in normal and cancer tissues.[23] MiR-635 is related to the progression of NSCLC.[24] Tai et al. explained that circ_0000735 promotes the progress of NSCLC through miR-635 / FAM83F axis.[25] In this study, miR-635 was decreased in NSCLC tissues or cells and mainly played an inhibitory role in NSCLC. Moreover, the

miRNA was regulated by circ_0102231 and its downregulation reversed circ_0102231 silencing-induced influence knockdown in NSCLC cells. This regulatory axis is reported for the first time.

Through TargetScan we confirmed that the downstream target protein of miR-635 was NOVA2. The NOVA family has two most important subtypes: NOVA2 and NOVA1.[26,27] NOVA2 has been considered as an oncogene that regulates the malignant progression of tumors.[28] The role of NOVA2 in NSCLC has been previously reported,[29,30] but its relationship with miR-635 has not been clarified. In this study, NOVA2 was abnormally high expressed in tumor tissues and cells. The introduction of NOVA2 could reverse the changes of cell function caused by miR-635. Considering the participation of the PI3K/AKT signaling pathway in NSCLC occurrence and progression,[31,32] we explored this pathway and proved that the activation of PI3K/AKT signaling pathway was regulated by circ_0102231/miR-635 axis.

In summary, this study discovered that circ_0102231 and NOVA2 expression levels were increased, while miR-635 expression was reduced in NSCLC tissues and cells. The absence of circ_0102231 hindered cell proliferation and angiogenesis but fortified the apoptosis through miR-635/NOVA2 pathway, which provides a possible avenue to explore in the treatment of NSCLC in the future.

In conclusion, based on the above studies, circ_0102231 absence could block tumor formation in vitro and in vivo. The regulatory networks between circ_0102231, miR-635 and NOVA2 have also been elucidated for the first time, which may be useful in studying the treatment of NSCLC.

AUTHOR CONTRIBUTIONS

Qiong Yu designed and supervised the study. Jianhong Liu conducted the experiments and drafted the manuscript. Xu Yang collected and analyzed the data, operated the software and edited the manuscript. All authors reviewed the manuscript.

CONFLICT OF INTEREST STATEMENT

The authors declare that they have no conflicts of interest.

DATA AVAILABILITY STATEMENT

The data used to support the findings of this study are available from the corresponding author upon request.

ORCID

Qiong Yu https://orcid.org/0009-0004-3323-7968

REFERENCES

1. Siegel RL, Miller KD, Jemal A. Cancer statistics, 2018. CA Cancer J Clin. 2018;68:7–30.
2. Bray F, Ferlay J, Soerjomataram I, Siegel RL, Torre LA, Jemal A. Global cancer statistics 2018: GLOBOCAN estimates of incidence and mortality worldwide for 36 cancers in 185 countries. CA Cancer J Clin. 2018;68:394–424.
3. Qin H, Wang F, Liu H, Zeng Z, Wang S, Pan X, et al. New advances in immunotherapy for non-small cell lung cancer. Am J Transl Res. 2018;10:2234–45.
4. Herbst RS, Morgensztern D, Boshoff C. The biology and management of non-small cell lung cancer. Nature. 2018;553:446–54.
5. Zhou R, Wu Y, Wang W, Su W, Liu Y, Wang Y, et al. Circular RNAs (circRNAs) in cancer. Cancer Lett. 2018;425:134–42.
6. Beermann J, Piccoli MT, Viereck J, Thum T. Non-coding RNAs in development and disease: background, mechanisms, and therapeutic approaches. Physiol Rev. 2016;96:1297–325.
7. de Almeida RA, Fraczek MG, Parker S, Delneri D, O'Keefe RT. Non-coding RNAs and disease: the classical ncRNAs make a comeback. Biochem Soc Trans. 2016;44:1073–8.
8. Qu S, Yang X, Li X, Wang J, Gao Y, Shang R, et al. Circular RNA: a new star of noncoding RNAs. Cancer Lett. 2015;365:141–8.
9. Enuka Y, Lauriola M, Feldman ME, Sas-Chen A, Ulitsky I, Yarden Y. Circular RNAs are long-lived and display only minimal early alterations in response to a growth factor. Nucleic Acids Res. 2016;44:1370–83.
10. Tan Z, Cao F, Jia B, Xia L. Circ_0072088 promotes the development of non-small cell lung cancer via the miR-377-5p/NOVA2 axis. Thorac Cancer. 2020;11:2224–36.
11. Li X, Yang L, Chen LL. The biogenesis, functions, and challenges of circular RNAs. Mol Cell. 2018;71:428–42.
12. Wang YG, Wang T, Ding M, Xiang SH, Shi M, Zhai B. Hsa_circ_0091570 acts as a ceRNA to suppress hepatocellular cancer progression by sponging hsa-miR-1307. Cancer Lett. 2019;460:128–38.
13. Jin Y, Li L, Zhu T, Liu G. Circular RNA circ_0102049 promotes cell progression as ceRNA to target MDM2 via sponging miR-1304-5p in osteosarcoma. Pathol Res Pract. 2019;215:152688.
14. Wang Q, Cang Z, Shen L, Peng W, Xi L, Jiang X, et al. circ_0037128/miR-17-3p/AKT3 axis promotes the development of diabetic nephropathy. Gene. 2021;765:145076.
15. Cao X, Li F, Shao J, Lv J, Chang A, Dong W, et al. Circular RNA hsa_circ_0102231 sponges miR-145 to promote non-small cell lung cancer cell proliferation by up-regulating the expression of RBBP4. J Biochem. 2021;169:65–73.
16. Hsu MT, Coca-Prados M. Electron microscopic evidence for the circular form of RNA in the cytoplasm of eukaryotic cells. Nature. 1979;280:339–40.
17. Qian C, Yang Y, Lan T, Wang Y, Yao J. Hsa_circ_0043265 restrains cell proliferation, migration and invasion of tongue squamous cell carcinoma via targeting the miR-1243/SALL1 Axis. Pathol Oncol Res. 2021;27:587130.
18. Tan J, Pan W, Chen H, du Y, Jiang P, Zeng D, et al. Circ_0124644 serves as a ceRNA for miR-590-3p to promote hypoxia-induced cardiomyocytes injury via regulating SOX4. Front Genet. 2021;12:667724.
19. Ma G, Li G, Fan W, Xu Y, Song S, Guo K, et al. Circ-0005105 activates COL11A1 by targeting miR-20a-3p to promote pancreatic ductal adenocarcinoma progression. Cell Death Dis. 2021;12:656.
20. Ge L, Shi R. Progress of EGFR-TKI and ALK/ROS1 inhibitors in advanced non-small cell lung cancer. Int J Clin Exp Med. 2015;8:10330–9.
21. Wang Y, Li L, Zhang W, Zhang G. Circular RNA circLDB2 functions as a competing endogenous RNA to suppress development and promote cisplatin sensitivity in non-squamous non-small cell lung cancer. Thorac Cancer. 2021;12:1959–72.
22. Wei D, Sun L, Feng W. hsa_circ_0058357 acts as a ceRNA to promote nonsmall cell lung cancer progression via the hsamiR243p/AVL9 axis. Mol Med Rep. 2021;23:470.
23. Zhang Y, Sun Z, Zhang Y, Fu T, Liu C, Liu Y, et al. The microRNA-635 suppresses tumorigenesis in non-small cell lung cancer. Biomed Pharmacother. 2016;84:1274–81.
24. Zhu D, Yu Y, Wang W, Wu K, Liu D, Yang Y, et al. Long noncoding RNA PART1 promotes progression of non-small cell lung cancer cells via JAK-STAT signaling pathway. Cancer Med. 2019;8:6064–81.
25. Tai G, Zhang M, Liu F. Circ_0000735 enhances the proliferation, metastasis and glycolysis of non-small cell lung cancer by regulating the miR-635/FAM83F axis. Exp Lung Res. 2021;47:136–48.
26. Ule J, Stefani G, Mele A, Ruggiu M, Wang X, Taneri B, et al. An RNA map predicting Nova-dependent splicing regulation. Nature. 2006;444:580–6.

27. Xiao H. MiR-7-5p suppresses tumor metastasis of non-small cell lung cancer by targeting NOVA2. Cell Mol Biol Lett. 2019;24:60.
28. Li G, Zhao C, Zhang H, Yu J, Sun Y, Zhang Y. Hsa_circ_0046263 drives the carcinogenesis and metastasis of non-small cell lung cancer through the promotion of NOVA2 by absorbing Mir-940 as a molecular sponge. Cancer Manag Res. 2020;12:12779–90.
29. Yi S, Li Z, Wang X, Du T, Chu X. Circ_0001806 promotes the proliferation, migration and invasion of NSCLC cells through miR-1182/NOVA2 Axis. Cancer Manag Res. 2021;13:3067–77.
30. Li C, Liu H, Niu Q, Gao J. Circ_0000376, a novel circRNA, promotes the progression of non-small cell lung cancer through regulating the miR-1182/NOVA2 network. Cancer Manag Res. 2020;12:7635–47.
31. Sun B, Hu N, Cong D, Chen K, Li J. MicroRNA-25-3p promotes cisplatin resistance in non-small-cell lung carcinoma (NSCLC) through adjusting PTEN/PI3K/AKT route. Bioengineered. 2021;12:3219–28.
32. Guan L, Zhang L, Wang T, Jia L, Zhang N, Yan H, et al. POM121 promotes proliferation and metastasis in non-small-cell lung cancer through TGF-beta/SMAD and PI3K/AKT pathways. Cancer Biomark. 2021;32:293–302.

How to cite this article: Liu J, Yu Q, Yang X. Circ_0102231 inactivates the PI3K/AKT signaling pathway by regulating the miR-635/NOVA2 pathway to promote the progression of non-small cell lung cancer. Thorac Cancer. 2023;14(35):3453–64. https://doi.org/10.1111/1759-7714.15138